On the Link between Tropical Cyclones and Daily Rainfall Extremes Derived from Global Satellite Observations

OLIVIER P. PRAT

Cooperative Institute for Climate and Satellites, North Carolina State University, and NOAA/National Centers for Environmental Information, Asheville, North Carolina

BRIAN R. NELSON

Center for Weather and Climate, NOAA/NESDIS/NCEI, Asheville, North Carolina

(Manuscript received 7 April 2016, in final form 29 June 2016)

ABSTRACT

The authors evaluate the contribution of tropical cyclones (TCs) to daily precipitation extremes over land for TC-active regions around the world. From 1998 to 2012, data from the Tropical Rainfall Measuring Mission (TRMM) Multisatellite Precipitation Analysis (TMPA 3B42) showed that TCs account for an average of 3.5% ± 1% of the total number of rainy days over land areas experiencing cyclonic activity regardless of the basin considered. TC days represent between 13% and 31% of daily extremes above 4 in. day^{-1}, but can account locally for the large majority (>70%) or almost all (≈100%) of extreme rainfall even over higher-latitude areas marginally affected by cyclonic activity. Moreover, regardless of the TC basin, TC-related extremes occur preferably later in the TC season after the peak of cyclonic activity.

1. Introduction

Tropical cyclones (TCs) contribute significantly to precipitation over impacted land areas (e.g., Cry 1967; Milton 1980; Larson et al. 2005; Knight and Davis 2007; Nogueira and Kleim 2011; Dare et al. 2012; Prat and Nelson 2013a,b; Brun and Barros 2014; Ng et al. 2015, among others). In addition to bringing an important influx of freshwater over land, TCs are often associated with extreme rainfall regardless of the metric considered (Kim et al. 2006; Wu et al. 2007; Knight and Davis 2009; Konrad and Perry 2010; Barlow 2011; Kunkel et al. 2011; Villarini and Denniston 2016). For instance, records for 3-day (3929 mm) and 4-day (4869 mm) rainfall accumulation were established on the island of La Réunion by Tropical Cyclone Gamede in 2007 (Quetelard et al. 2009). For comparison, Gamede's 4-day record accumulation represents about 50% of the maximum average annual rainfall for the African continent (Table 1).

Previous work investigated TC contribution to precipitation budgets over land using satellite data from the TRMM Multisatellite Precipitation Analysis (Huffman et al. 2007) for 1) the southeastern United States and 2) basins around the world for the period 1998–2009 (Prat and Nelson 2013a,b). The present study, a companion paper, aims to complement the aforementioned work by analyzing the TC contribution to extreme daily rainfall. The first section describes the datasets and methodology. In the second section, we present the global TC contribution to extreme rainfall over land. The final section summarizes the key findings. Results for selected locations around the world are also provided (Table 2).

2. Data and methodology

The TRMM Multisatellite Precipitation Analysis (TMPA 3B42 version 7), which combines remotely sensed microwave (TMI, SSM/I, AMSR, and AMSU; expansions of acronyms are available online at http://www.ametsoc.org/PubsAcronymList) and calibrated IR estimates with gauge analyses, provides 3-hourly/0.25° precipitation estimates for 50°S–50°N (Huffman et al. 2007). The dataset allows for monitoring the tropical

---

Corresponding author address: Dr. Olivier P. Prat, Cooperative Institute for Climate and Satellites-NC (CICS-NC), North Carolina State University, and NOAA/National Centers for Environmental Information, 151 Patton Avenue, Asheville, NC 28801.
E-mail: opprat@ncsu.edu

DOI: 10.1175/JCLI-D-16-0289.1

TABLE 1. Highest average annual precipitation extremes for each domain selected (source: NCEI). Values used as wet millimeter days (WMMD).

Domain	Highest daily average (mm day^{-1})	Place	Country	Elevation (m)	Number of years of record
NCA	24.62	Quibdo	Columbia	37	16
SEA	32.50	Mawsynram	India	1401	38
SWA	32.50	Mawsynram	India	1401	38
OCE	23.64	Bellenden Ker	Australia	1555	9
EAF	28.16	Debundscha	Cameroon	9	32

cyclone activity from genesis to decay and from the tropical belt to higher latitudes.

Tropical cyclone tracks are taken from the International Best Track Archive for Climate Stewardship (IBTrACS; Knapp et al. 2010). The IBTrACS database gathers historical records of tropical cyclones from various official meteorological agencies worldwide. IBTrACS provides information regarding the nature of the storm, the center location, and the intensity of the TC every 6 h. The TC center location and characteristics (sustained wind speed, pressure) are linearly interpolated every 3 h to match the temporal resolution of the satellite observations. Satellite precipitation events occurring within a 500-km radius centered over the TC location are identified as tropical cyclone rainfall (Rodgers et al. 2001; Larson et al. 2005; Lau et al. 2008; Jiang and Zipser 2010; Prat and Nelson 2013a,b). Following the TC along its track allows accounting for landfalling cyclones and cyclones staying offshore yet coming close enough to the coast, producing subsequent rainfall over land. To assess the contribution of tropical cyclones to extreme rainfall, we considered the five continental domains used previously (Prat and Nelson 2013b). They are identified as North and Central America (NCA), Southeast and East Asia (SEA), South and West Asia (SWA), Oceania (OCE), and East Africa (EAF). Figure 1 displays the delineation of the domains along with the TC basins' locations (I–VI). This study spans a 15-yr period from 1998 to 2012. Slight to moderate differences from previous work (Prat and Nelson 2013b) are to be expected for TC rainfall and TC contribution due to the longer period of study and the random and infrequent nature of TCs.

3. TC global contribution to precipitation budget and extreme events

Figure 1 displays the annual average precipitation for TC rainfall (Fig. 1a). The precipitation associated with TCs indicates higher accumulation for Southeast and East Asia (880 mm yr^{-1}) and North and Central America over the Pacific coast of Mexico (504 mm yr^{-1}) (Fig. 1b). Over land, the maximum TC rainfall is 202 mm yr^{-1} (Gracias a Dios Department, Honduras), 781 mm yr^{-1} (Ilocos Region, Philippines), 159 mm yr^{-1} (Odisha State, eastern India), 277 mm yr^{-1} (Melville Island, Australia), and 295 mm yr^{-1} (Toamasina Province, eastern Madagascar) for NCA, SEA, SWA, OCE, and EAF respectively. Overall, the NCA domain has the highest cyclonic activity (34 TCs per year) followed by SEA, OCE, SWA, and EAF with respectively 70%, 43%, 27%, and 22% of the NCA activity. The number of events in relation with TCs is more important (>15 days yr^{-1}) offshore Mexico's mainland Pacific Coast and over the South China and Philippine Seas (Fig. 1b). The number of wet millimeter days (WMMD; Shepherd et al. 2007), which is the number of days exceeding the highest daily rainfall average for each domain (Table 1), is significant over the same aforementioned areas (Mexico's coast, southern China, and the Philippine Sea) with comparable number of events for NCA and SEA. For an increasing daily threshold of 2 in. day^{-1} (1 in. ≈ 25.4 mm, EPD2 threshold; Karl et al. 1995), a similar pattern is observed with maxima over the same regions of NCA and SEA (Fig. 1d). However, pattern differences are found for daily accumulation above 4 in. day^{-1} (EPD4 threshold; Barlow 2011), with higher counts found for SEA over the South China and Philippine Seas (Fig. 1e).

Figure 2 displays the TC contribution for rainfall totals (Fig. 2a), rainfall events (Fig. 2b), and extreme rainfall events (Figs. 2c–e). We note that global TC rainfall patterns are consistent with similar studies (Shepherd et al. 2007; Jiang and Zipser 2010), with differences in TC rainfall (Fig. 1a) and TC contributions (Fig. 2a) being due to a different duration (Prat and Nelson 2013b) and/or to the fact that we consider an annual basis rather than a seasonal basis (Shepherd et al. 2007; Jiang and Zipser 2010). The maximum TC contribution over land is 50% (southern Baja California), 37% (southeastern Taiwan), 45% (southern Oman), 40% (western Australia), and 29% (southwestern Madagascar) for the various domains (Fig. 2a). Some of the largest TC contributions are observed over arid areas (southern Baja California, western Australia, and Arabian Peninsula). While the first two regions

TABLE 2. Annual TC rainfall (mean, max), and average number of rainy days (All and TC) with maximum annual TC ratio for different threshold (WMMD, EPD2, and EPD4) and for 50 selected locations. Numbers in boldface indicate maximum values (by domain and metric).

		TC Rainfall (%)		All			WMMD			EPD2			EPD4		
				Number (day yr^{-1})		Max	Number (day yr^{-1})		Max	Number (day yr^{-1})		Max	Number (day yr^{-1})		Max
	City	Mean	Max	All	TC	(%)	All	TC	(%)	All	TC	(%)	All	TC	(%)
NCA	Houston (Texas)	7.2	22.3	92.7	2.6	8.0	17.5	1.3	19.0	**7.0**	0.6	22.2	1.1	0.2	66.7
	New Orleans (Louisiana)	6.4	17.9	155.7	4.1	4.9	18.2	1.6	20.5	6.5	0.9	36.4	1.0	0.1	**100**
	Miami (Florida)	8.9	28.8	113.5	4.6	9.9	18.7	2.0	34.2	5.2	1.1	60.6	0.6	0.3	**100**
	Key West (Florida)	14.0	44.5	105.4	5.1	12.9	11.1	2.0	51.0	4.2	1.3	72.0	0.7	0.3	83.3
	Charleston (South Carolina)	6.9	19.6	104.5	4.2	9.7	15.2	1.3	25.4	3.7	0.7	68.4	0.4	0.1	**100**
	Wilmington (North Carolina)	8.2	22.5	110.8	4.0	7.3	17.8	1.6	21.8	5.5	0.8	40.0	1.0	0.4	**100**
	New York (New York)	3.5	12.8	95.7	1.5	5.9	15.3	0.8	16.1	4.3	0.4	29.2	0.3	0.1	**100**
	Mexico City (Mexico)	2.9	10.7	**193.5**	3.5	3.5	5.1	0.3	28.6	0.3	0.1	**100**	0	0	0
	Tampico (Mexico)	7.7	31.7	91.9	3.2	8.7	14.0	1.5	38.1	5.1	0.8	56.5	1.1	0.2	80.0
	Merida (Mexico)	5.6	15.9	101.1	4.7	10.9	10.9	0.9	25.5	2.6	0.3	33.3	0.1	0	**100**
	La Paz (Mexico)	**37.1**	**69.8**	53.7	4.6	**18.9**	1.5	0.9	**100**	0.5	0.4	**100**	0.2	0.2	**100**
	Puerto Vallarta (Mexico)	8.0	14.1	120.6	**8.8**	13.4	14.8	2.1	28.2	3.1	0.7	52.6	0.3	0.1	**100**
	Guadalajara (Mexico)	2.9	5.6	123.4	3.9	6.8	6.8	0.2	13.9	0.5	0	0	0	0	0
	Acapulco (Mexico)	13.1	25.0	96.9	7.2	13.3	17.2	**3.5**	40.3	6.5	**1.8**	60.9	1.2	**0.5**	**100**
	Oaxaca (Mexico)	6.0	15.4	129.2	5.1	9.1	12.3	1.0	24.5	2.3	0.4	61.5	0.1	0.1	**100**
	Havana (Cuba)	8.5	29.4	124.9	5.4	12.1	15.9	1.7	30.1	4.1	0.8	88.9	0.6	0.2	**100**
	Port-au-Prince (Haiti)	7.7	26.1	138.4	4.2	8.7	14.7	1.3	35.3	3.7	0.7	60.0	0.7	0.4	**100**
	Santo Domingo (Dominican Republic)	10.2	24.0	134.0	5.1	10.4	17.9	2.3	31.3	4.8	1.3	53.8	0.5	0.3	**100**
	Guatemala City (Guatemala)	3.3	12.5	188.6	3.2	6.9	16.2	0.6	13.4	2.3	0.3	52.9	0.3	0.1	**100**
	Tegucigalpa (Honduras)	3.7	15.9	131.8	3.4	4.9	12.9	0.8	27.6	1.5	0.1	35.7	0.1	0	50.0
	Managua (Nicaragua)	4.2	30.0	134.4	2.0	3.9	17.2	0.8	17.5	4.0	0.3	38.5	0.6	0.2	85.7
	Nassau (Bahamas)	8.1	22.2	120.4	4.2	8.3	12.4	1.3	33.3	4.0	0.5	66.7	0.8	0.2	**100**
	San Juan (Puerto Rico)	8.5	18.7	151.4	4.2	5.3	15.6	1.6	24.5	4.7	0.9	63.6	1.1	0.3	**100**
	Pointe-à-Pitre (Guadeloupe)	10.6	31.3	162.3	4.8	5.3	12.7	2.0	49.0	4.6	1.2	71.4	0.9	0.2	**100**
	Fort-de-France (Martinique)	9.7	29.8	155.0	4.5	5.8	8.8	1.2	39.0	2.4	0.5	75.0	0.4	0.1	**100**
	Kingston (Jamaica)	9.9	26.8	145.5	4.2	7.5	**20.6**	2.3	27.6	6.9	1.3	45.2	**1.6**	**0.5**	66.7
SEA	Osaka–Kobe–Kyoto (Japan)	7.7	21.5	120.6	4.6	11.1	13.7	1.7	33.3	5.6	1.1	46.4	0.8	0.3	85.7
	Tokyo–Yokohama (Japan)	8.3	16.7	134.4	4.6	7.5	13.2	1.9	26.1	6.7	1.4	52.4	1.1	0.4	**100**
	Taipei (Taiwan)	**24.2**	**45.3**	122.4	11.0	**15.5**	15.7	4.3	**53.1**	8.9	3.0	60.0	2.3	1.3	**100**
	Guangzhou–Foshan–Shenzhen (China)	10.9	23.6	110.5	8.3	13.2	17.4	2.2	26.6	9.7	1.4	36.7	1.7	0.4	61.5
	Shanghai (China)	5.5	27.8	116.1	2.9	5.8	7.9	0.7	33.3	3.2	0.4	53.3	0.4	0.1	**100**
	Fuzhou (China)	12.4	31.5	105.0	7.5	13.3	13.2	2.0	34.0	6.3	1.4	55.0	0.9	0.3	**100**
	Busan (South Korea)	7.9	17.6	95.9	4.5	10.6	13.8	1.9	30.0	7.7	1.3	47.8	1.7	0.3	**100**
	Seoul–Incheon (South Korea)	7.4	18.4	79.5	2.8	10.6	13.9	1.6	34.8	7.8	1.1	47.1	2.5	0.4	63.6
	Ho Chi Min (Vietnam)	1.3	11.9	144.7	1.6	6.4	13.5	0.4	32.7	4.5	0.03	20.0	0.3	0	0
	Manila (Philippines)	18.2	32.6	151.9	**12.5**	13.9	**22.5**	**5.5**	43.2	**11.9**	**4.1**	**64.1**	**3.4**	**1.4**	**100**
	Guam (United States)	9.6	30.9	**191.4**	6.7	10.3	11.8	1.8	41.3	5.6	1.1	59.4	1.0	0.3	**100**
SWA	Dhaka (Bangladesh)	4.0	13.4	108.8	2.2	4.1	**20.3**	1.0	14.6	**11.2**	**0.8**	19.7	**2.2**	**0.4**	60.0
	Kolkata (India)	6.2	17.0	103.7	**3.2**	6.9	15.9	**1.2**	21.3	8.0	**0.8**	25.0	1.5	0.2	**100**
	Chennai (India)	8.8	27.2	90.7	2.6	7.4	10.0	1.0	35.5	5.4	**0.8**	44.4	1.2	0.3	66.7
	Colombo (Sri Lanka)	1.3	14.1	**158.1**	1.4	4.4	19.1	0.3	11.1	8.0	0.2	21.6	0.8	0.1	87.5
	Karachi (Pakistan)	4.9	25.7	32.0	0.6	**11.5**	1.6	0.1	**100**	0.9	0.1	28.6	0.2	0	0
	Masqat (Oman)	**15.4**	**62.1**	21.1	0.3	7.5	0.6	0.2	85.7	0.3	0.2	**100**	0.02	0.02	**100**
OCE	Port Hedland (Australia)	**34.0**	**76.4**	40.4	6.0	**25.9**	4.9	1.8	**100**	1.9	0.9	**100**	0.3	0.2	**100**
	Darwin (Australia)	12.6	33.4	118.6	**6.9**	16.4	**25.0**	**3.3**	30.1	**7.7**	**1.6**	53.6	1.3	0.3	**100**
	Port Moresby (Papua New Guinea)	1.5	8.8	**151.3**	1.7	5.8	19.0	0.4	11.6	3.9	0.1	23.1	0.3	0	0
	Nouméa (New Caledonia)	5.6	17.1	93.3	2.2	5.5	15.0	0.9	22.6	5.3	0.5	44.4	0.9	0.2	80.0
EAF	St Denis (Réunion)	**15.4**	**48.6**	128.8	5.3	**12.1**	5.0	1.2	**69.2**	2.0	0.5	**100**	0.5	0.1	**100**
	Antananarivo (Madagascar)	8.6	22.8	**132.8**	**6.2**	11.0	**13.0**	**1.5**	40.0	2.8	**0.6**	76.9	0.1	0.1	**100**
	Beira (Mozambique)	4.4	17.2	64.4	1.8	9.6	12.3	0.7	24.4	**5.7**	0.2	19.0	1.1	0.1	37.5

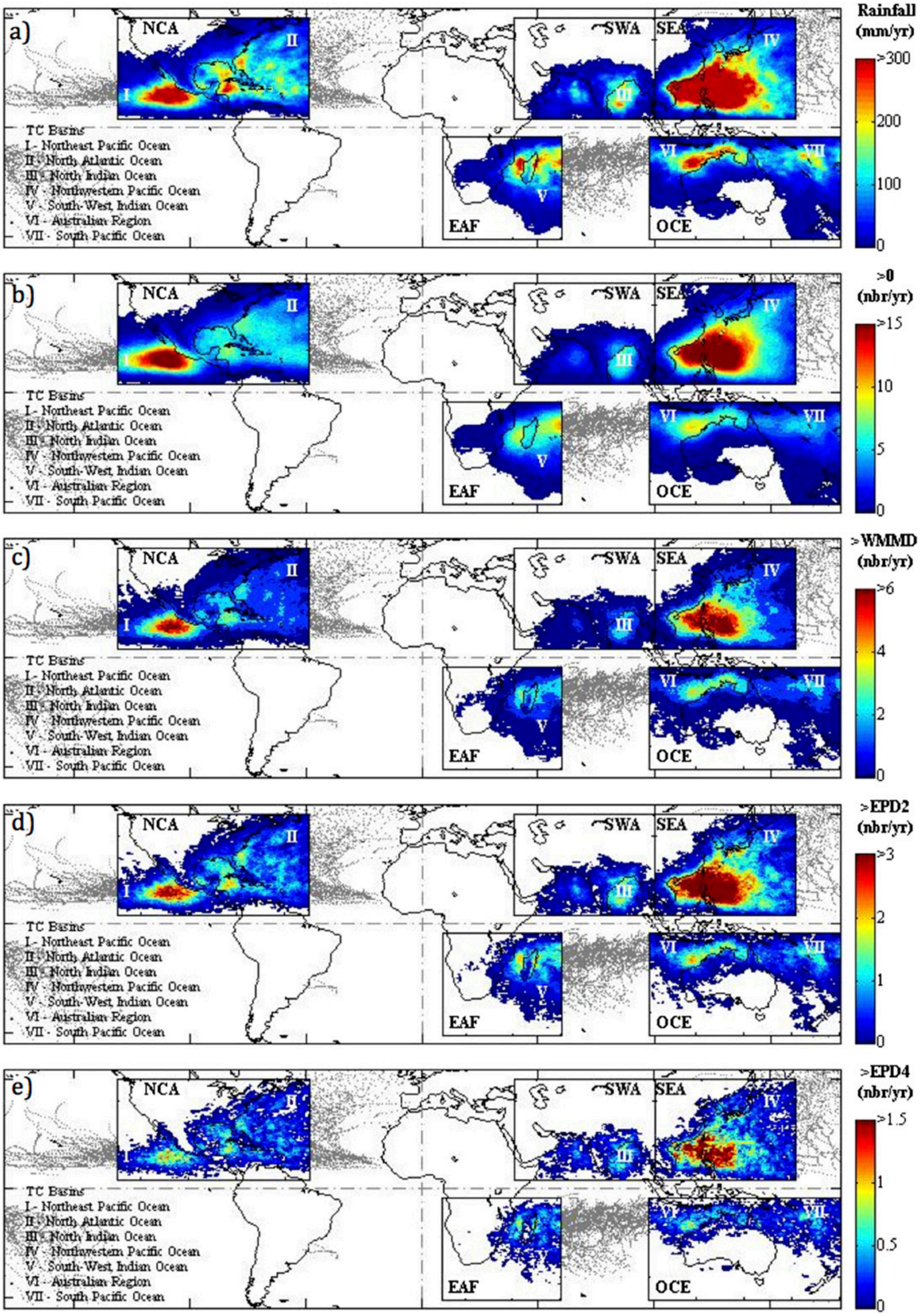

FIG. 1. (a) Average annual TC rainfall. Average annual TC number of rainy days with rainfall: (b) $R > 0$, (c) $R >$ WMMD, (d) $R > 2$ in. day^{-1} (EPD2), and (e) $R > 4$ in. day^{-1} (EPD4).

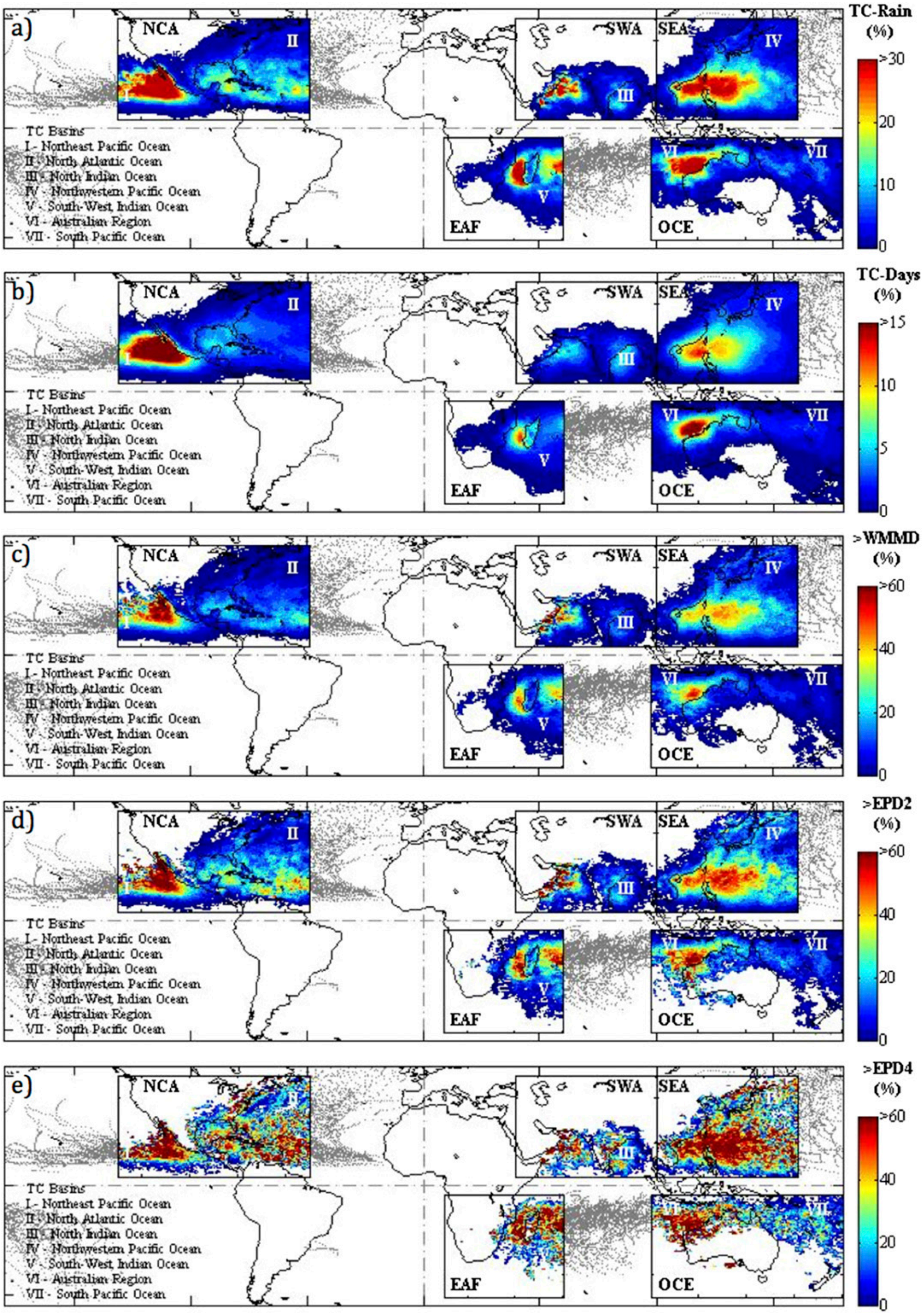

FIG. 2. (a) TC average annual contribution, and TC contribution to daily rainfall: (b) $R > 0$, (c) $R >$ WMMD, (d) $R >$ 2 in. day^{-1} (EPD2), (e) $R >$ 4 in. day^{-1} (EPD4).

experience relatively regular cyclonic activity, the Arabian Peninsula, despite exposure to a lesser cyclonic activity from the north Indian Ocean basin (~1/4 of NCA), presents a high contribution (45%), which is principally associated with Cyclone Keila (2010). Globally, we find a similar spatial distribution between the number of TC events (Fig. 2b) and the TC contribution (Fig. 2a). Because tropical storms are generally associated with more intense precipitation, the TC contribution is higher than the corresponding proportion of TC days. For NCA, while tropical cyclones account locally for between 2% (East Coast and Gulf of Mexico) and 20% (Baja California and Mexico Pacific coast) of precipitation days (Fig. 2b), they represent from 10% (southeastern United States, Atlantic coast, and Caribbean) to over 60% of WMMD (Fig. 2c) and over 80% of EPD2 for Baja California (Fig. 2d). In addition, TCs represent more than 50% of EPD4 over Florida and the coastal Carolinas and account for almost all of EPD4 for Baja California (Fig. 2e). Furthermore, even over areas where TCs are infrequent, such as New England (Keim et al. 2007), they can be responsible for more than 70% of EPD4 (Fig. 2e). For SEA, SWA, OCE, and EAF, the maximum proportion of TC days is respectively about 17%, 8%, 20%, and 18% locally (Fig. 2b). The local maxima for WMMD are about 50%–60% for SEA, OCE, and EAF and 80% for SWA over the Arabian Peninsula (Fig. 2c). The proportion of WMMDs related to TC activity represents a threefold increase with respect of the total number of TC days for SEA, OCE, and EAF (Fig. 2a). For SWA, the increase is about tenfold locally, and is due to a marginal TC activity over the arid Arabian Peninsula (Fig. 2c). Clusters of TC extremes are localized near Oman's easternmost point and over southern Oman and bear the signature of Cyclones Gonu in 2007 (Dube et al. 2009; Abdalla and Al-Abri 2011) and Keila in 2010 respectively. Locally, TCs account for more than 80% of EPD4 events even for higher-latitude areas seldom experiencing TCs (northwestern China) or over areas farther inland in central India along the Satpura Range (Fig. 2e). A similar situation is found for OCE with an important ratio of TC-related EPD4 in northern and western Australia. The results obtained for WMMD (Fig. 2c), EPD2 (Fig. 2d), and EPD4 (Fig. 2e) are consistent with recent studies that used in situ data (see Fig. 4 in Villarini and Denniston 2016). Similarly, we found that EPD4 associated with TCs accounted for more than 60% over northwestern Australia (Fig. 2e). Although each domain displays comparable trends and similar quantitative results for TC contribution to extreme precipitation events, the spatial distribution of extreme events is intertwined with TC activity and local climatological and geographical characteristics (arid, tropical, specific precipitation regimes).

Figure 3 quantifies the TC contribution over land (annual minimum, average, and maximum). The average (maximum) annual TC contribution computed for a given year over the land area impacted by TCs is 5.3% (7.0%), 7.2% (8.9%), 4.4% (8.8%), 7.6% (11.1%), and 8.6% (17.8%) for NCA, SEA, SWA, OCE, and EAF, respectively. NCA presents the largest land area impacted by TCs at an annual average of 5.5 × 10^6 km^2, an annual maximum of 8.7 × 10^6 km^2, and a total area impacted of 9.9 × 10^6 km^2 for 1998–2012. SEA presents a smaller area with an annual average of 4.6 × 10^6 km^2 followed by OCE, SWA, and EAF with 3.2, 2.3, and 1.4 × 10^6 km^2 respectively. On average, TCs represent 2.7% (SWA), 3.1% (NCA), 3.7% (SEA), 4.1% (OCE), and 4.4% (EAF), respectively, of the total number of rainy days. Regardless of the domain, the proportion of TC days remains relatively small but the proportion of extreme events linked to TC activity increases with increasing daily rainfall (WMMD, EPD2, and EPD4). More specifically, extremes rainfall linked with TC activity accounts for 4.5%–12%, 9%–18%, and 13%–30% of the total for WMMD, EPD2, and EPD4 respectively for the five domains. There is a five- to

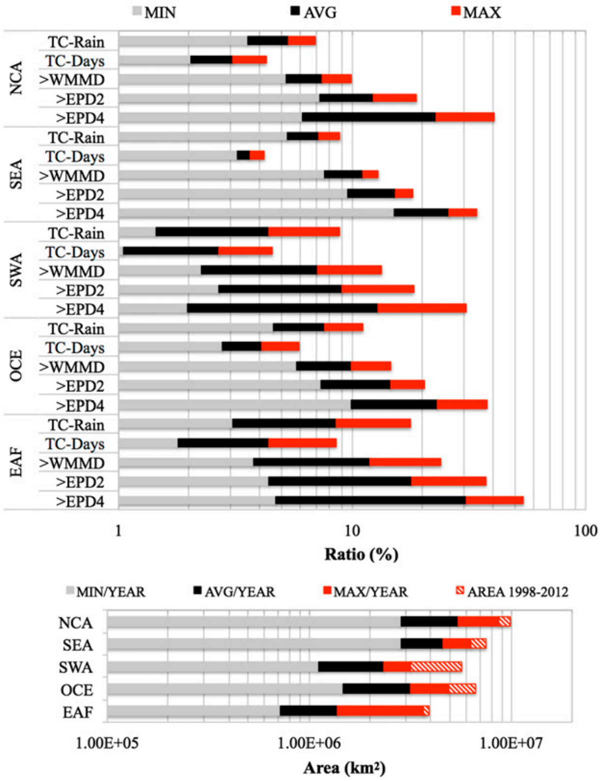

FIG. 3. (top) TC contribution and percentage of TC-rainfall over land for different daily thresholds (WMMD, EPD2, and EPD4) for the different domains (NCA, SEA, SWA, OCE, and EAF). The figure indicates the minimum (MIN), average (AVG), and maximum (MAX) contributions computed over the areas experiencing annual cyclonic activity over the period 1998–2012. (bottom) The minimum (MIN/YEAR), average (AVG/YEAR), and maximum (MAX/YEAR) area impacted on an annual basis and the maximum extend of the area impacted for the period 1998–2012 (AREA 1998–2012).

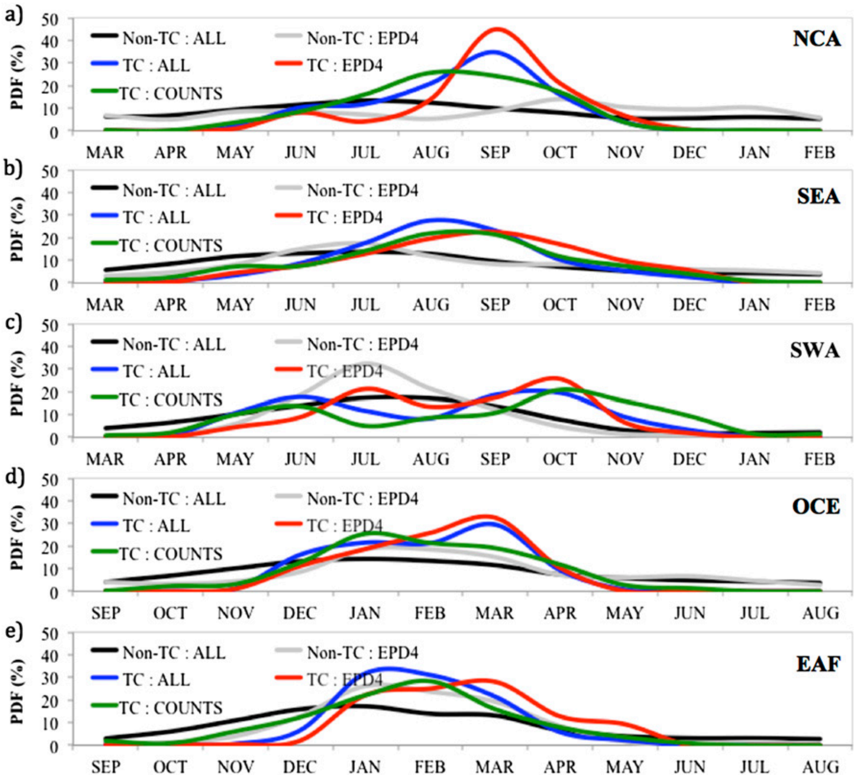

FIG. 4. Monthly distribution for all rainfall (>0 mm day^{-1}) and extreme rainfall events (EPD4) for non-TC and TC precipitation. Only areas experiencing cyclonic activity for the period 1998–2012 are included in the statistics. Plots are centered over the months of maximum TC activity. The average monthly TC activity is also reported.

eightfold increase between the proportion of daily TC counts (2.7%–4.4%) and the EPD4 ratio (13%–31%) associated with TCs. For a given year, 31% (SWA) and up to 54% (EAF) of EPD4 are attributed to TCs. With the lowest average land area impacted of 1.4 × 10^6 km^2 (maximum of 3.7 × 10^6 km^2), and despite the lowest TC activity (Prat and Nelson 2013b), the EAF domain has the highest TC rainfall contribution and systematically the highest proportion of TC rainfall days and daily extremes regardless of the intensity (WMMD, EPD2, and EPD4) both in terms of annual average and maxima.

Figure 4 displays the monthly distribution of non-TC and TC precipitation days and EPD4. The TC activity (green line) exhibits the characteristic bell-shaped curve with maximum in August–October for the Northern Hemisphere (NCA, SEA) and January–March for the Southern Hemisphere (OCE, EAF). The majority of the TC activity (55%–67%) occurs over the three aforementioned months. For the India domain (SWA), the TC activity is divided between the monsoon transition months in May–June (24%) and the end of the wet season in September–November (47%). Moreover, while the TC activity was mostly concentrated over the 6-month periods of June–November for the Northern Hemisphere (96% for NCA, 84% for SEA) and November–April for the Southern Hemisphere (94% for OCE, 93% for EAF), it was only 71% during the typical TC season (May–June and October–January) for the north Indian Ocean basin. For NCA, the maximum for non-TC rainfall happens in July whereas more EPD4 events occur in October (Fig. 4a). Overall, the NCA domain is characterized by a homogeneous distribution of non-TC rain events throughout the year with a monthly repartition ranging between 5% and 14%, which is comparable with non-TC extremes (Fig. 4a). The maximum observed in October for EPD4 events is consistent with previous work (Higgins et al. 2011; Prat and Nelson 2014) that showed that extratropical cyclones, synoptic-scale fronts, topography, and large-scale ascent were responsible for extreme precipitation, especially in October (Higgins et al. 2011). For TC rain, the maximum number of TC days (35%) is found in September, which also corresponds to the maximum (45%) of extreme precipitation events associated with TCs. Finally, we observe a higher proportion of extremes (EPD4) later in the TC season (September–November) than at the beginning (June–August). A possible explanation is that rising sea surface temperatures throughout the TC season would generate more intense storms and associated precipitation. A similar situation is observed for SEA, with the maximum for non-TC events and non-TC extreme events (EPD4) occurring in July and corresponding to the active phase of the East Asian summer monsoon (Chen et al. 2004) (Fig. 4b). August exhibits the highest number of TC days (28%) whereas September has the most TC extremes (22.5%). As for NCA, more extreme TC events (EPD4) happen later in the season (October–November).

Because of the monsoon regime, the SWA domain displays a strong contrast for non-TC rainfall between the winter monsoon (December–February) with a monthly repartition between 1.8% and 2.3% and the summer monsoon (May–September) with monthly repartition between 10% and 17% (Fig. 4c). Moreover, the difference between winter and summer monsoons is stronger for non-TC extreme events with 1.5% (December–February) and 91% (May–September) respectively (Fig. 4c). The months of September–October display the highest number of TC days (19%) with a maximum for extreme TC rain (26%) peaking later in October (Fig. 4c). For OCE, non-TC events range monthly from 4% to 14% and non-TC extremes from 3% to 19%, with a maximum in January (Fig. 4d). Again, we observe a higher proportion of extreme TC events (69%) later during the TC season (February–April) of the Southern Hemisphere. Furthermore, the peak for TC extremes is observed in March at the end of the TC season, and accounts for one-third of all TC related extremes. Finally, for EAF, the differences between the cooler dry season (May–October) and the hot wet season (November–April) are more pronounced than for OCE, with 78% of non-TC precipitation occurring during the wet season corresponding to almost all (94%) of non-TC extreme precipitation (Fig. 4e). The maximum of TC days (32%) happens in January and the maximum of TC-related extremes (28%) happens later in March as observed for OCE.

4. Summary and conclusions

This study investigated the link between tropical cyclone activity and extreme daily rainfall. Results show that for over land areas experiencing cyclonic activity, TC days account for 2.7%–4.4% of precipitation on an annual basis for the five domains. Regardless of the domain, the proportion of extreme events originating from tropical cyclones increases with increasing daily precipitation threshold. TC rainfall represents on average between 13% (SWA) and 31% (EAF) of EPD4 on an annual basis and up to 31% (SWA) and 54% (EAF) for record years. For specific locations and times TCs account for the majority of extreme rainfall events. For North America, TCs account for more than half (>50%–70%) of EPD4 along the U.S. Atlantic coast from Florida to New England and for almost all (~100%) EPD4 over Baja California. Similarly, TC-related rainfall represents over 70% of the extreme rainfall for East Asia (Taiwan, the east coast of China, and northwestern China), southern and western Asia (Oman and Satpura Mountains in India), Oceania (western and northern Australia), and East Africa (Mozambique's coast, Madagascar, and Reunion Islands). Results show that TC-related rainfall extremes (EPD4) are more frequent later in the season after the peak of cyclonic activity.

Acknowledgments. This research was supported by NOAA through the Cooperative Institute for Climate and Satellites–North Carolina under Cooperative Agreement NA14NES432003. The authors are grateful to Ken Knapp for helping with the internal review process and two anonymous reviewers for valuable comments and suggestions.

REFERENCES

Abdalla, O., and R. Y. Al-Abri, 2011: Groundwater recharge in arid areas induced by tropical cyclones: Lessons learned from Gonu 2007 in Sultanate of Oman. *Environ. Earth Sci.*, **63**, 229–239, doi:10.1007/s12665-010-0688-y.

Barlow, M., 2011: Influence of hurricane-related activity on North American extreme precipitation. *Geophys. Res. Lett.*, **38**, L04705, doi:10.1029/2010GL046258.

Brun, J., and A. P. Barros, 2014: Mapping the role of tropical cyclones on the hydroclimate of the southeast United States: 2002–2011. *Int. J. Climatol.*, **34**, 494–517, doi:10.1002/joc.3703.

Chen, T.-C., S.-Y. Wang, W.-R. Huang, and M.-C. Yen, 2004: Variation of the East Asian summer monsoon rainfall. *J. Climate*, **17**, 744–762, doi:10.1175/1520-0442(2004)017<0744:VOTEAS>2.0.CO;2.

Cry, G. W., 1967: Effects of tropical cyclone rainfall on the distribution of precipitation over the eastern and southern United States Environmental Science Services Administration Professional Paper 1, 67 pp.

Dare, R. E., N. E. Davidson, and J. L. McBride, 2012: Tropical cyclone contribution to rainfall over Australia. *Mon. Wea. Rev.*, **140**, 3606–3619, doi:10.1175/MWR-D-11-00340.1.

Dube, S. K., I. Jain, A. D. Rao, and T. S. Murty, 2009: Storm surge modelling for the Bay of Bengal and Arabian Sea. *Nat. Hazards*, **51**, 3–27, doi:10.1007/s11069-009-9397-9.

Higgins, R. W., V. E. Kousky, and P. Xie, 2011: Extreme precipitation events in the south-central United States during May and June 2010: Historical perspective, role of ENSO, and trends. *J. Hydrometeor.*, **12**, 1056–1070, doi:10.1175/JHM-D-10-05039.1.

Huffman, G. J., and Coauthors, 2007: The TRMM Multisatellite Precipitation Analysis (TMPA): Quasi-global, multiyear, combined-sensor precipitation estimates at fine scales. *J. Hydrometeor.*, **8**, 38–55, doi:10.1175/JHM560.1.

Jiang, H., and E. D. Zipser, 2010: Contribution of tropical cyclones to the global precipitation from eight seasons of TRMM data: Regional, seasonal, and interannual variations. *J. Climate*, **23**, 1526–1543, doi:10.1175/2009JCLI3303.1.

Karl, T. R., R. W. Knight, and N. Plummer, 1995: Trends in high-frequency climate variability in the twentieth century. *Nature*, **377**, 217–220, doi:10.1038/377217a0.

Keim, B. D., R. A. Muller, and G. W. Stone, 2007: Spatiotemporal patterns and return periods of tropical storm and hurricane strikes from Texas to Maine. *J. Climate*, **20**, 3498–3509, doi:10.1175/JCLI4187.1.

Kim, J.-H., C.-H. Ho, M.-H. Lee, J.-H. Jeong, and D. Chen, 2006: Large increase in heavy rainfall associated with tropical cyclone landfalls in Korea after the late 1970s. *Geophys. Res. Lett.*, **33**, L18706, doi:10.1029/2006GL027430.

Knapp, K. R., M. C. Kruk, D. H. Levinson, H. J. Diamond, and C. J. Neumann, 2010: The International Best Track Archive for Climate Stewardship (IBTrACS). *Bull. Amer. Meteor. Soc.*, **91**, 363–376, doi:10.1175/2009BAMS2755.1.

Knight, D. B., and R. E. Davis, 2007: Climatology of tropical cyclone rainfall in the Southeastern United States. *Phys. Geogr.*, **28**, 126–147, doi:10.2747/0272-3646.28.2.126.

——, and ——, 2009: Contribution of tropical cyclones to extreme rainfall in the southeastern United States. *J. Geophys. Res.*, **114**, D23102, doi:10.1029/2009JD012511.

Konrad, C. E., II, and L. B. Perry, 2010: Relationships between tropical cyclones and heavy rainfall in the Carolina region of the USA. *Int. J. Climatol.*, **30**, 522–534, doi:10.1002/joc.1894.

Kunkel, K. E., D. R. Easterling, D. A. R. Kristovich, B. Gleason, L. Stoecker, and R. Smith, 2011: Recent increases in U.S. heavy precipitation associated with tropical cyclones. *Geophys. Res. Lett.*, **37**, L24706, doi:10.1029/2010GL045164.

Larson, J., Y. Zhou, and R. W. Higgins, 2005: Characteristics of landfalling tropical cyclones in the United States and Mexico: Climatology and interannual variability. *J. Climate*, **18**, 1247–1262, doi:10.1175/JCLI3317.1.

Lau, K. M., Y. P. Zhou, and H. T. Wu, 2008: Have tropical cyclones been feeding more extreme rainfall? *J. Geophys. Res.*, **113**, D23113, doi:10.1029/2008JD009963.

Milton, D., 1980: The contribution of tropical cyclones to the rainfall of tropical Western Australia. *Singapore J. Trop. Geogr.*, **1**, 46–54, doi:10.1111/j.1467-9493.1980.tb00101.x.

Ng, B., K. Walsh, and S. Lavender, 2015: The contribution of tropical cyclones to rainfall in northwest Australia. *Int. J. Climatol.*, **35**, 2689–2697, doi:10.1002/joc.4148.

Nogueira, R. C., and B. D. Kleim, 2011: Contributions of Atlantic tropical cyclones to monthly and seasonal rainfall in the eastern United States 1960–2007. *Theor. Appl. Climatol.*, **103**, 213–227, doi:10.1007/s00704-010-0292-9.

Prat, O. P., and B. R. Nelson, 2013a: Precipitation contribution of tropical cyclones in the southeastern United States from 1998 to 2009 using TRMM satellite data. *J. Climate*, **26**, 1047–1062, doi:10.1175/JCLI-D-11-00736.1.

——, and ——, 2013b: Mapping the world's tropical cyclone rainfall contribution over land using the TRMM Multi-satellite Precipitation Analysis. *Water Resour. Res.*, **49**, 7236–7254, doi:10.1002/wrcr.20527.

——, and ——, 2014: Characteristics of annual, seasonal, and diurnal precipitation in the Southeastern United States derived from long-term remotely sensed data. *Atmos. Res.*, **144**, 4–20, doi:10.1016/j.atmosres.2013.07.022.

Quetelard, H., P. Bessemoulin, R. S. Cerveny, T. C. Peterson, A. Burton, and Y. Boodhoo, 2009: World-record rainfalls during tropical cyclone Gamede. *Bull. Amer. Meteor. Soc.*, **90**, 603–608, doi:10.1175/2008BAMS2660.1.

Rodgers, E. B., R. F. Adler, and H. F. Pierce, 2001: Contribution of tropical cyclones to the North Atlantic climatological rainfall as observed from satellites. *J. Appl. Meteor.*, **40**, 1785–1800, doi:10.1175/1520-0450(2001)040<1785:COTCTT>2.0.CO;2.

Shepherd, J. M., A. Grundstein, and T. L. Mote, 2007: Quantifying the contribution of tropical cyclones to extreme rainfall along the coastal southeastern United States. *Geophys. Res. Lett.*, **34**, L23810, doi:10.1029/2007GL031694.

Villarini, G., and R. F. Denniston, 2016: Contribution of tropical cyclones to extreme rainfall in Australia. *Int. J. Climatol.*, **36**, 1019–1025, doi:10.1002/joc.4393.

Wu, Y., S. Wu, and P. Zhai, 2007: The impact of tropical cyclones on Hainan Island's extreme and total precipitation. *Int. J. Climatol.*, **27**, 1059–1064, doi:10.1002/joc.1464.